Journal of Multidisciplinary Engineering Science and Technology (JMEST)
ISSN: 2458-9403
Vol. 6 Issue 1, January - 2019

A Study of a Multi-Thresholding Segmentation Algorithm Based on Bio-Inspired Meta-Heuristic and Non-Extensive Tsallis Statistics

Paulo S. Rodrigues *, Murillo F. Bouzon, Miller Horvath, Victor Varella, Guilherme A. Wachs-Lopes
Computer Science Department
Centro Universitario FEI
São Bernardo do Campo
*Correspondence Author: psergio@fei.edu.br

Abstract—An image segmentation process is one of the most important steps in an image recognition or analysis application pipeline. It is a step that splits each image into disjointed regions of interest. It is also a task that is usually performed by biological processes, such as human visual system. Due to the low processing and ease of implementation, one of the most used techniques is the thresholding method, which consists in finding the best cutting thresholds of a probability distribution histogram. However, the higher the number of thresholds, the greater the computational complexity. And there is no consensus on the number of thresholds and the partitioning position as well. This paper presents a study of the number of thresholds for segmenting an image into their regions of interest. For this purpose, the proposed method uses a bio-inspired algorithm based on meta-heuristics, called firefly with a non-extensive Tsallis statistics kernel. Also, the images are pre-filtered with a low-pass filter based on a *q*-gaussian function. Using a manually segmented database, the results show that there is an inverse correlation between the Fourier spectrum of an image and the number of thresholds which most approximates the image from the used ground truth. This suggests an automatic method for calculating the required number of thresholds.

Keywords—SIFT, Tsallis Statistics, Non-Extensive Statistics, Multi-thresholding Image Segmentation, Fire-Fly segmentation

I. INTRODUCTION AND RELATED WORKS

In Computer Science, more specifically in computer vision area, image segmentation is the process of splitting and image into its regions of interest based on a clustering criteria. One of the oldest methods that has been widely applied in that process is the so called thresholding by histogram, which considers that the optimal separation of a probability distribution of intensities is highly correlated with the division of the image itself in regions of interest. This assumption is accepted but has limitations since, although it makes a thresholding technique somehow simple, it is a source of errors, especially because a histogram of intensities does not carry spatial information, what we known is an essential information given the analysis and interpretation of scanned scenes. However, such techniques have often been used to be simple to implement and easily understandable. In addition, many practical applications showed good results in using this type of technique, having special attention from researchers. The optimal thresholding problem (OTP), has been extensively investigated by several researchers for decades. Among the techniques studied are those based on entropy, an old concept proposed by L. Boltzmann under the context of thermodynamics to explain the relationship between work and energy. Years later, C. Shannon adapted the Boltzmann's ideas to measure the amount of information in a communication channel. Since then, this concept has been applied with great recognition in various areas of science.

The general idea behind the concept of entropy for image segmentation is that under an ideal threshold, there is the maximum transference of information between the region of interest and its background. This idea was used firstly by T. Pun [1] in order to achieve two levels of intensity maps, assuming that the optimal threshold is that one which maximizes the additivity property of Shannon entropy. This property states that the entropy of a whole physical system (represented by its probability distribution) can be computed by the sum of its individual subsystems (represented by their individual probability distributions).

Kapur et al. [2] maximized the superior entropy threshold value for the optimal threshold, and Abutaleb [3] improved this method using two-dimensional entropies. In addition, the Work of Li and Lee [4] and Pal [5] used the Kullback-Leibler divergence to select the optimal threshold, and Sahoo et al. [6] used the Reiny entropy aiming the same goal. More details about these approaches can be found in [7], a review about entropy methods for image segmentation.

Considering the constraints of the traditional Shannon entropy, in [8] M. P. Albuquerque and colleagues proposed an image segmentation method based on entropy Non-extensive Tsallis statistics [9], a new type of entropy that has been considered as a generalization of Shannon entropy, which includes a

real parameter q, called Non-extensive parameter. Since the pioneer work of Albuquerque work, a vast literature was presented demonstrating promising performance of this method applied to optimal thresholding problem. More practical systems have been emerged under this theory, and recent works such as [10], [11], [12] and [13] has demonstrated the efficiency of the non-extensive Tsallis entropy applied to image segmentation in Computed Aided Diagnosis for medical images, the so called CAD systems.

However, the main constraint of this approach is the calculation of the parameter q, empirically chosen for most of the works. In [14] was shown a correlation between the gray intensity probability distribution and the value of this parameter, suggesting a first proposal for its calculation.

The OTP for two levels of thresholds, the so-called image binarization, has been used in applications to extract objects (the first layer) from its background (the second layer). It can also be observed in tracking systems, commonly used in video and images. However, even when the task is a simple object extraction from its background, one may need to use more than one level of segmentation, due to the presence of noise and other artifacts. This is the multi-thresholding task. In [12] and [13] presented a methodology combining the Tsallis entropy and mathematical morphology to achieve three levels of thresholding under low SNR (signal-to-noise ratio). Later in [15], it was suggested that two segmentation levels may be sufficient for the separation of the main regions in natural scenes. The results were compared with manually segmented images of a database systematically built as a ground-truth. The proposed method has the advantage of multi-segmentation, also called multi-level thresholding Problem (MLTP) in linear time, recursively splitting the regions of interest.

Recursive segmentation opposes to free splitting, in the sense that the latter chooses a partition at the highest levels regardless of the amount and the localization of regions in the prior lower levels, while in the recursive segmentation, each achieved sub-region is splitted again to form the next levels. Then, the recursive segmentation is dependent on the amount and location of regions found in lower levels. However, in the recursive strategy there is no guarantee that the thresholding in multi-levels leads to a desired division because different regions that co-existed at the same level *r* cannot co-exist anymore (or are entirely incorporated at different levels) when the same region is divided into *r*+1 levels. Thus, some authors have investigated the image segmentation process based on free thresholding on multi-levels. The disadvantage of this process is the computational time that is not linear requiring an order of complexity of $O(L^{d+1})$ to derive *d* thresholds *L n* intensity levels, which is unacceptable, of course, even for *d* = 2 in the case of segmentation in three levels used in applications that require real time.

Thus, some authors have proposed the use of bio-inspired meta-heuristics to find various thresholds in a process of multi-segmentation. See, for example, [16] and references therein for a review.

Therefore, the development of meta-heuristics has gained much attention from researchers, particularly in the last decade, when a variety of such algorithms has been applied to various NP-Complete problems. Some of the best known meta-heuristics are genetic algorithms [17], simulated annealing [18], Tabu search [19], optimization by ant colony [20], and particle swarm optimization [17], [22].

In turn, firefly algorithm is a bio-inspired meta-heuristic based on the fireflies behavior following their luminescence. The work of Lukasik and Zak [23] and Yang [24] suggested that the methods based on firefly meta-heuristic outperform other major existing meta-heuristics. Recently, M. Horng [25] proposed the use of this algorithm in a thresholding approach using as objective function the minimization of cross-Entropy for multi-level thresholding. This is the same objective function proposed by P. Yin in [22]. The general conclusion was that the method based on the cross-entropy, a linear timing algorithm, reached threshold values near to the exhaustive algorithm based on the same entropic kernel.

When it comes to natural image segmentation, the optimal number of thresholds for better segmentation is still an open issue in the literature; therefore, it is considered a subjective choice and very dependent of deep cognitive processes still unknown to researchers. Moreover, the correlation of the various parameters involved in several stages is still a process somewhat poor addressed, where the majority of methodologies are tested with parameters set previously in an intuitive way.

The optimal number of thresholds for better segmentation of a natural image is still an open issue in the literature about and is therefore considered a subjective choose and very dependent of deep cognitive processes still unknown to re- searchers. Moreover, the correlation of the various parameters involved in the several stages, is still a process somewhat poor addressed, where the majority of methodologies are tested with parameters set previously empirically.

This paper proposes the study of the parameterization of the bio-inspired meta-heuristic Firefly for multi-thresholding segmentation of natural images, especially regarding the number of thresholds that better approximates an automatic segmentation from a corresponding manual contour. The kernel of the proposed algorithm is based on non-extensive Tsallis entropy.

Finally, due to the large set of parameters, the computation of these parameters is achieved in a parallel and distributed architecture programming. Among the main results obtained, we find that there is a strong correlation between the homogeneity of the image regions and the number of used thresholds that approaches the automatic segmentation from a corresponding manual segmentation.

The remainder of this paper is organized as the following. In Section 2 all theoretical foundations are described. Then, Section 3 introduces the images database. Next, in Section 4, the similarity measure

function used in the experiments is presented. Later, Section 5 describes the proposed experiments and presents the results. Finally, Section 6 reviews the main results of the paper and give directions on future researches.

II. Theoretical Foundations

A. Non-Extensive Multi-Segmentation

In this section, we review the concept of non-extensive Tsallis entropy and show its application as a kernel in the Firefly algorithm for image segmentation. An extensive analytical, experimental and comparative review of this topic can be found in the paper of Rodrigues [16], which shows that the firefly meta-heuristic has a better performance in multi-threading applications under a kernel based on Tsallis entropy. The concept of entropy is fundamental in the remarkable work of Shannon, which proposes the popular equation of
Shannon's entropy in the field of information theory:

$$S = \sum pi \log pi \quad (1)$$

where *pi* is a probability of a physical system to occur in a state *i* and $\sum pi = 1.0$, $0 \leq pi \leq 1.0$.

This entropy definition is more accurately applied to traditional physical systems, which are called Extensive Physical Systems since their future physical properties can be predictably scaled from the state and interaction of their current elements. However, for over a century, it is well known that this equation cannot describe precisely systems whose elements have long-range interactions in temporal and space terms. Such systems are called Non-Extensive Physical Systems [9] and have recently been gaining great attention from researchers. For these cases, C. Tsallis has proposed a new formalism [9], developed through the Tsallis's entropy, given by the following equation:

$$S = \frac{1-\sum p_i^q}{q-1} \quad (2)$$

where q is the real (entropic) parameter. This idea, although relatively new, has been well accepted in the scientific community, and has been successfully applied to various areas of science such as hydrodynamics (turbulent systems), astronomy (speed of galaxies), economics, biochemistry, social interactions, image processing, and many others. A comprehensive reference with applications and more details of this formalism can be found in [9].

It can be proved that Tsallis' entropy is a generalization of the Shannon's since Equation (2) reduces to Equation (1) in the limit when the variable q tends to 1 [26]. The work [8] was the first one to apply the Tsallis Entropy for segmentation of natural scenes. Later generalization of the Shannon's since Equation (2) reduces to Equation (1) in the limit when the variable q tends to 1 [26]. The work [8] was the first one to apply the Tsallis Entropy for segmentation of natural scenes. Later, Rodrigues et al in [15] and [27] presented the first methods for automatic computation of parameter q for segmentation tasks.
In [28], [29], [30] it is shown that the Firefly algorithm performs better if the objective function is based on non-extensive Tsallis entropy. The Firefly algorithm, proposed by Xin-She Yang in [24], is a meta-heuristic inspired by the behavior of fireflies, which are attracted one by another according to their natural luminescence. In the end, the convergence is reached generating clusters of fireflies, where the brighter ones attract the other fireflies under certain restrictions, such as: (1) all fireflies are unisex so that one firefly will be attracted to any other firefly; (2) attractiveness is proportional to brightness, thus a less bright firefly will move towards a brighter one. If a particular firefly is the brighter one, then it will move randomly.
The general idea is modeling a non-linear optimization problem by associating each problem's variable to a firefly and make the objective evaluation depending on these variables, which are associated to the fireflies brighten. Then, iteratively, the variables are updated (their brightness) under pre-setting rules until the convergence to a global minimum. Generically, it is accomplished at each generation, according to the following main steps:

- Bright evaluation;
- Compute all distances between each pair of fireflies;
- Move all fireflies one toward all others, according to their brightness;
- Keep the best solution (the brighter firefly);
- Generate randomly new solutions;

The kernel of the algorithm is its evaluation function, denoted here by *Z*, which influences the final result very much and depends on the current problem. Specifically, for multi-level thresholding problem, as proposed in [28], [25] and [24], each firefly is considered a d-dimensional variable, where each dimension is a distinct threshold, partitioning the histogram space into *d* + 1 distinct regions. It was shown experimentally in [25] and [24] that the achieved results, though not optimal, are consistent with the corresponding results of brute-force algorithms. However, the objective function used in the methods followed an extensive formalism, considering the equation for the cross entropy.

In the specific case found in [28], the goal is to minimize an objective function *Z* that is based on non-extensive Tsallis entropy and its pseudo-additivity property, given by:

$$S_q(A \oplus B) = S_q(A) + S_q(B) + (1 - q)S_q(A)S_q(B) \quad (3)$$

where *A* and *B* are two statistically independent physical systems, $S_q(A)$ and $S_q(B)$ are computed by Equation (2), and $S(A \oplus B)$ is the total entropy of the non-extensive physical system composed by *A* and *B*.

In this work, the *Z* function is defined according to Equation 3. Then, the number of physical states is the

number of chosen partitions. Therefore, for two partitions (binary segmentation) the evaluation function of firefly algorithm for the firefly fi is defined as:

$$Z(f_i) = S_q(P_1 \oplus P_2) = S_q(P_1) + S_q(P_2) + (1 - q)S_q(P_1)S_q(P_2) \quad (4)$$

In the case of *d* partitions the *Z* function is defined as:

$$Z(f_i) = S_q(P_1 \oplus P_2 \ldots P_d) = S_q(P_1) + S_q(P_2) + \ldots + S_q(P_d) + (1 - q)\, S_q(P_1)S_q(P_2)\ldots S_q(P_d) \quad (5)$$

Thus, the brightness of each firefly f_i is directly proportional to the value of Equation (5).

The superior result of Tsallis Entropy is only possible due to the introduction of the non-extensive parameter q, which gives to the optimization method more flexibility in finding a better solution. The firefly algorithm is described in details in [16], where the authors demonstrate the efficiency of this strategy applied to generic images.

B. *The q-gaussian Filtering*

As the Expression (2) is presented as one generalization of the Expression (1), the Statistical Mechanics also states defines, under the same ideas, a generalization to the Gaussian function, denoted here as q-Gaussian. In [31], for example, a generic q-gaussian function was defined as:

$$g_q(x) = \frac{\sqrt{\beta}}{C_q}\, e_q^{-\beta x^2}, \quad (6)$$

where β = 1/(3 - q), e_q^n is an exponential function and C_q is a normalization constant.

As the *q*-entropy, the *q*-exponential function uses the non-extensive parameter q as a traditional deformation as well.

The function e_q^n was defined in [31] as an analogous expression to e^x, given by $[1 + (1 - q)x]^{\frac{1}{1-q}}$, where the limits are:

$$e_q^x \begin{cases} [1 + (1 - q)x]^{\frac{1}{1-q}}, for\ q \neq 1\ and\ 1 + (1-q)x > 0 \\ 0, \quad for\ q \neq 1\ and\ 1 + (1-q)x \leq 0 \\ e^x, \ for\ q = 1 \end{cases} \quad (7)$$

The normalization factor C_q is also dependent of the non-extensive parameter q, as the following:

$$C^q \begin{cases} 2\sqrt{\pi}\Gamma\left(\frac{1}{1-q}\right) \frac{1}{(3-q)\sqrt{1-q}\,\Gamma\left(\frac{3-q}{2(1-q)}\right)}, for\ -\infty < q < 1 \\ \sqrt{\pi}, \quad for\ q = 1 \\ \sqrt{\pi}\Gamma\left(\frac{(3-q)}{2(q-1)}\right) \frac{1}{\sqrt{q-1}\,\Gamma\left(\frac{1}{(q-1)}\right)}, \ for\ 1 < q < 3 \end{cases} \quad (8)$$

The gamma function Γ(n) = $(n - 1)!$ is an extension of factorial function in the complex domain.

Considering the Equation (6), we can define an analogous to two-dimensional *q*-gaussian, defined as:

$$g_q(y) = \frac{\sqrt{\beta}}{C_q}\, e_q^{-\beta y^2}, \quad (9)$$

Besides, in the work of Borges [31] it was defined the product of two variables in the non-extensive domain, called as *q*-product, given by:

$$x \oplus_q y \equiv [x^{1-q} + y^{1-q} - 1]_+^{\frac{1}{1-q}} \quad (10)$$

In the work of [32], a 2D q-gaussian was defined as a product of the two q-exponentials (6) and (9) in the domain defined by Expression (10), in the following way:

$$G_q(x, y) = g_q(x) \oplus_q g_q(y) \quad (11)$$

$$G_q(x, y) = [g_q(x)^{1-q} + g_q(y)^{1-q} - 1]^{\frac{1}{1-q}} \quad (12)$$

In [31] and references therein in found the q-product theory in a more detailed way.

Finally, we can define a 2D q-gaussian as:

$$G_q(x, y) = \left[\left(\frac{\sqrt{\beta}}{C_q}\, e_q^{-\beta x^2}\right)^{1-q} + \left(\frac{\sqrt{\beta}}{C_q}\, e_q^{-\beta y^2}\right)^{1-q} - 1\right]^{\frac{1}{1-q}} \quad (13)$$

To get the traditional gaussian function, we can compute the limit of Expression (11) when $q \rightarrow 1$.

In Fig. 1 six topologies are presented and three discretizations of the 2D *q*-Gaussians built according to Equation (11). In this figure, each function presents a different q-value. In this paper, we have tested five different topologies according to the set q = {0.1, 0.75, 2.0, 2.5, 2.99} as a pre-processing of the input images in order to verify the impact of each topology under six different thresholds. Also, we have tested the set q = {0.1, 0.5, 0.35, 0.75, 0.99} as entropic kernels of the proposed firefly meta-heuristic.

III. Experimental Database

In the experiments of this work we have used 300 images of a database from the Berkeley University. These images are natural images from several classes, and each image was manually segmented given contours of their regions. The task of image segmentation is an open problem, and we can highlight two reasons: (*i*) a correct segmentation depends on the image context as well as the human point of view, and (*ii*) it is rare to find an image database manually segmented to formally compare results. The Berkeley database is the most known to this purpose. Consequently, the researches show their results throughout few images and highlight what they believe are the correct under an intuitive way. So, it is evident that the same methodology works with other image of the same class. However, the remaining question is: what is a correct segmentation?

Under lack of a response, it is needed at least a reference point so that the comparison between several techniques under the same database or parameterization can be plausible. In this sense, the image database used in this work can be considered an attempt to establish such a reference.

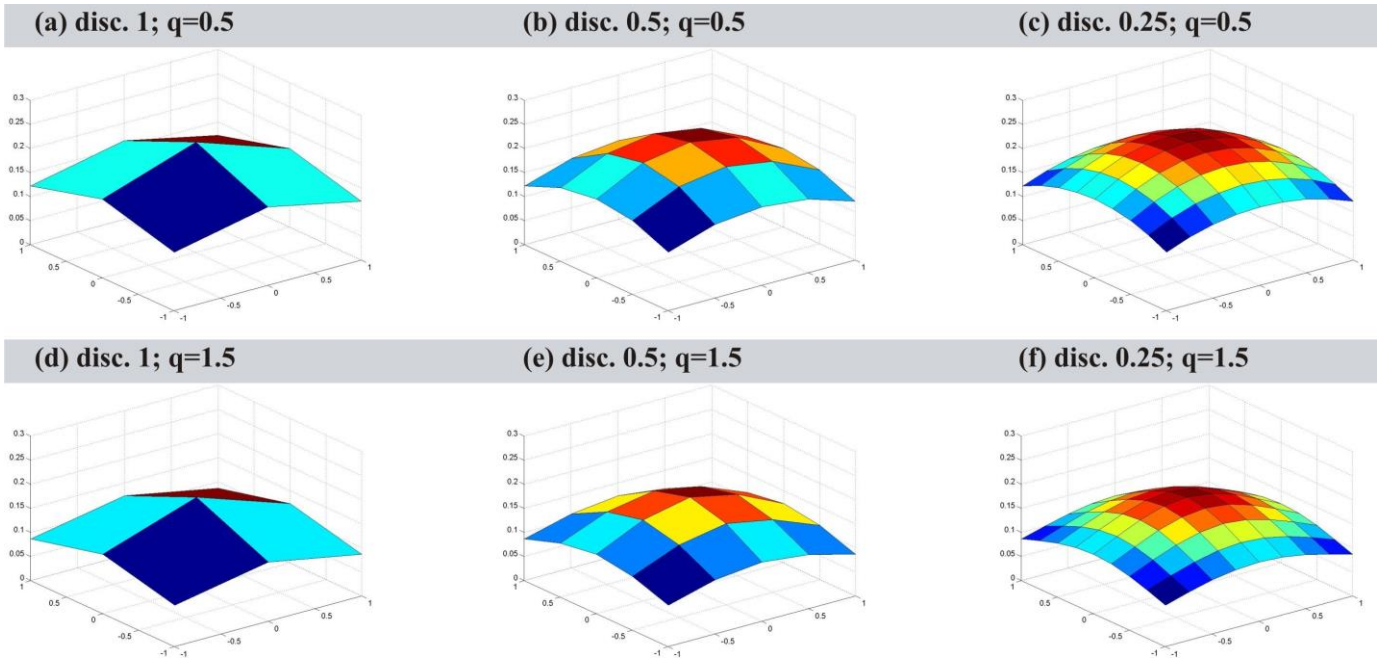

Fig. 1. Graphics of six 2D *q*-gaussians with the corresponding q-values under three different discretizations.

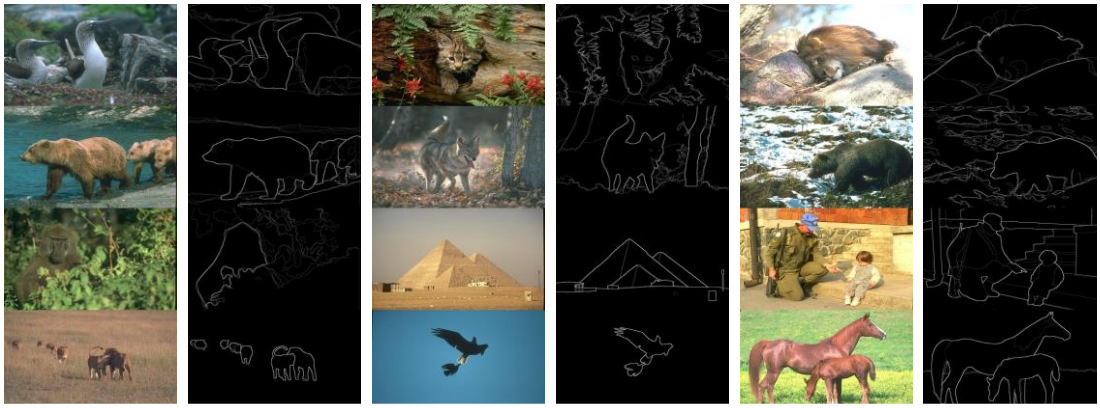

Fig. 2. Twelve examples (columns 1, 3 and 5) of the original images and their corresponding manual segmentations (columns 2, 4, and 6).

Fig. 2 shows twelve examples (first, third and fifth columns) of images of this database and their corresponding manual segmentations (second, fourth and sixth columns, respectively), where it is possible to note the high degree of consistence between the segmentation accomplished by different peoples. For further details on this database, see [33].

IV. Similarity Measure

We defined a function to measure the similarity between the manual and the automatic segmentation. However, this is a difficult task and the problem is still unsolved. Sezgin and Sankur [34] proposed 5 quantitative criterias for measuring the luminance region and shaped 20 classical methods to measure the similarity between them. But the criteria they proposed was not based on a golden standard defined set of images, thus the method of comparison proposed in [34] can be used only as an intrinsic quality evaluation of the segmented areas: i.e, one output image segmented into uniformly molded regions cannot be considered as close as expected to the manual segmentation.

On the other hand, similarity measures based on some ground-truth are not easy to propose when the system needs to detect several regions in an image, a common task in computational vision. Moreover, the comparison of several related regions is a challenging process since not only the edge is difficult to measure but also its spatial location. Also, in the area of computer vision, is an important demand to be able to deduct regions that are interrelated.

Although it is possible to design an algorithm which tolerates localization errors, it is likely that detecting only the matching pixels and assuming all others are flaws or false positive and may provide a poor performance.

One can speculate from Figure 2 that the comparison between the edge-maps derived from the automatic and manual segmentations must tolerate localization errors as long as there are also divergences on the edges of the golden standard. Thus, the consideration of some differences can be useful in the final result as shown in [33].

On the other hand, from 2D edge-maps, such as the one we used, one can obtain two types of information: geometrical dispersion and intensity dispersion. The geometric dispersion measures the size and the location of the edges; the intensity dispersion measures how common is that edge among all manual segmentations that were overlapped. Thus, the geometric dispersion between two edge-maps has its information measured in a quantitative manner, in the *x* and *y* dimensions, while the luminance dispersion can be represented by the *z* dimension.

The divergence of information between the two edge-maps of an M × N image in the *x* dimension is calculated by the Euclidean distance between the two maps (i.e. the M_x as vertical projection at the edge map for automatic segmentation and the H_x is the corresponding vertical projection for the manual one). So, in this article, we propose an evaluation function between the two edge-vertical-projection M_x and H_x of the *x* dimension presented in (14) to measure how far the automatically-obtained segmentation is from the manual one in this specific direction:

$$Sim_x(M_x|H_x) = \sqrt{\sum_M \left(M_x(i) - H_x(i)\right)^2} \quad (14)$$

where M_x and H_x are the image edges projections in the *x* direction, manual and automatic respectively.

Similarly, the corresponding functions are proposed respectively for *y* (15) and *z* (16) directions:

$$Sim_y(M_y|H_y) = \sqrt{\sum_N \left(M_y(i) - H_y(i)\right)^2} \quad (15)$$

$$Sim_z(M_z|H_z) = \sqrt{\sum_L \left(M_z(i) - H_z(i)\right)^2} \quad (16)$$

where *N* e *L* are the sizes of *y* e *z* distributions (for horizontal and luminance distribution, respectively). Note that *N* is the image resolution on the *y* dimension and *L* is the total of gray levels (i.e. 256).

Thus, in this study, we propose the following evaluation function to measure the similarity between two edge-maps:

$$Sim(M|H) \quad = Sim_x + Sim_y + Sim_z \quad (17)$$

V. Experiments And Discussion

A. Experimental Methodology

Clearly, we can note that the size of parameter set is considerably large here, as is typical in applications of digital signal processing, especially in the case of multi-stage architectures as is easily found in mid-level machine vision applications. The process of image segmentation is a typical example. On the other hand, there are rare works in computer science and neuroscience literature studying each parameter relating them to the subjective interpretation of an image. Generally, most works in the area choose to set previously the parameter values and empirically demonstrate the performance of the methods through a final comparison with other methods under these fixed values.

Thus, the work proposed here is intended to be a small step toward the study of the relationship of some parameters to a process considered purely cognitive, as is the interpretation of the main regions of an image by a human being, represented here by the manual segmentation of Berkeley database. If there is any relationship between a parameter and the natural image partition, a first step to ravel these relationships is obviously the statistical observation of the parameter behavior and the given manual segmentation. Thus, in this paper, we chose to automatically vary the set of parameters involved in the automatic segmentation and observe the results against the corresponding manual segmentation.

An intuitive observation which corroborates this strategy is that in case of multi-thresholding, the number of considered regions by the most manual segmentation should not be an increasing nor decreasing function regarding scene complexity. Since the number of thresholds is directly proportional to the number of found regions, the number of used thresholds in a manual segmentation should be low. Thus, one of the studied parameters here was the number of thresholds. The first experiments indicate this direction, as shown in Figs. 4 and 5.

The results observed in Figs. 4 and 5 intrigue and lead directly to the obvious question of what image features (cognitive or not), an image must have to be better segmented by few (1 or 2, for example) or several (more than 2) thresholds. We have not found in the related literature any work addressing this issue. Thus, in the experiments in this paper we propose the Fourier spectrum of an image as that feature which most likely has some correlation with the number of thresholds. It is known that as greater the amount of high frequencies embedded in an image, greater is the amount of details and possibly greater will be the number of optimal thresholds for segmenting it. Intuitively, the contrary can be also true. Thus, one of the experiments proposed here is to observe the Fourier spectrum in correlation with the number of optimal thresholds. The confirmation of this behavior may allow further applications that extract from the image information to enable the computation of the number of optimal thresholds to segment it.

To compute the large set of parameters of the involved algorithms, in the experiments carried out in this work we used distributed processing. Then, it was tested five values of the non-extensive parameter q = {0.1, 0.5, 0.35, 0.75, 0.99} in the kernel of FFA. In addition, each input image was pre-filtered with five different values of q = {0.1, 0.75, 2.0, 2.5, 2.99} in the q-gaussian filter and six different thresholds T = {1, 2, 3, 4, 5, 6} in FFA.

Fig. 3 shows the experimental flowchart used in this paper to study the parameterization of the proposed methodology. Each rectangle is labeled with a specific experimental methodology stage and the arrow is the data flow.

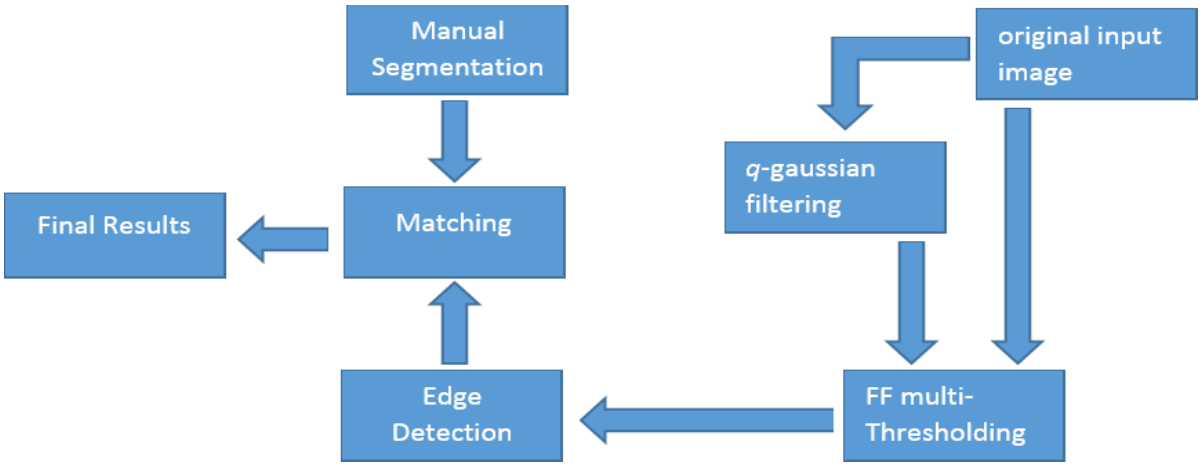

Fig. 3. Flowchart of the proposed experimental method.

The experimental flowchart has two inputs at different moments. Initially the entry original input image indicates the processing of an image that is filtered in q-gaussian filtering stage before moving to the FF multi-thresholding stage.

Note that the FF multi-thresholding stage can be accomplished also directly from original input image without the q-gaussian filtering. After the FF multi-thresholding stage, an edge detection based on sobel operator is carried out, which output is compared with the corresponding manual segmentation image in matching stage. The final results stage shows the results of comparison accomplished with Equation (17).

In this work, this flowchart has been tested for each of 300 images of original Berkeley database (Section III). Each input image can pass though the pre-filtering stage where a q-gaussian low-pass filter is applied for five values for q. This step is accomplished with Equation (13). Regarding the five values of q and the six different thresholds used in stage FF Multi-thresholding, each of 300 images pass 150 times through this flowchart. The whole process was, as already mentioned, automatic.

B. Results

As described before, the flowchart shown in Fig. 3 was used for experimental studies of this work and is automatically executed 150 times for each one of the 300 images of Berkeley database (Section III). For each image, it was taken the best parameter set up that led to the nearest multi-segmentation of the corresponding ground truth image (that manually segmented). So, each image has a number of thresholds which is considered optimal, minimizing the matching between the manual and automatic multi-thresholding. The histogram distribution of these thresholds for all 300 images can be seen in Fig. 4.

The distribution of Fig. 4 shows that the number of images that are better segmented with few thresholds (1, 2 and 3) is much higher than those which are segmented with higher number of thresholds (4, 5, and 6).

In turn, Fig. 5 shows a 10 × 10 matrix where each cell (*i, j*) is the average of all matching using Equation (17) for those images that are better segmented with *i* thresholds after a q-gaussian pre-filtering with $q = j$. For example, a cell (2, 0.5) is the average of all matching using Equation (17) for those images that are better segmented with 2 thresholds after a q-gaussian pre-filtering with q = 0.5, and cell (3, 1.0) is the average of all matching using Equation (17) for those images that are better segmented with 3 thresholds after a *q*- gaussian pre-filtering with q = 1.0, in this case this is the same as a pre-filtering with a traditional gaussian filtering, since q = 1.0. Also, all cells were normalized according the scale shown in the left vertical bar where the blue value is the best (lower) average matching and the red value is the worst (higher) average matching.

According to the color scale shown in Fig. 5, as bluer a cell is, lower is the distance matching between the manual and automatic image segmentation, and as redder a cell is, greater is this distance. Thus, this figure complements the results obtained in the distribution shown in Fig. 4, suggesting that as smaller the number of thresholds greater is the chance of achieving a closer matching to a manual segmentation.

The results shown in Figs. Figs. 4 e 5 demonstrate that the number of thresholds is low for most images of the Berkeley database. However, these results also raise up the question of which depends on the number of thresholds? Then we hypothesize that the number of thresholds depends on the distribution of the high and low frequencies embedded in an image. To demonstrate this hypothesis, was carried out experiments whose flowchart is shown in Fig. 6.

The general idea behind the experimental flowchart of Fig. 6 is that to measure the information of the image's features and correlate that information with the number of thresholds that reaches the best segmentation with the FF algorithm. Since the number of image details give an idea of how homogeneous is that image, we compute its Fourier transform, measure the frequency spectrum and correlate it with the

number of thresholds that minimize the distance between the automatic and manual segmentation.

Thus, for each image I_{xy} from the Berkeley database that has been better segmented with *L* thresholds we compute the Fourier transform $\mathcal{F}(I_{xy})$ for I_{xy} . The output is then converted to the Fourier spectrum *P* ($\mathcal{F}(I_{xy})$), given by Equation (18).

$$P\left(\mathcal{F}(I_{xy})\right), \ = |\mathcal{F}(I_{xy})| = R^2(u,v) + J^2(u,v) \quad (18)$$

where *R* is the real part and *J* is the imaginary part of the Fourier spectrum.

Finally, consider that R_I^L is the real term of the Fourier spectrum of the image *I* which was best segmented with *L* thresholds. If the number of images with *L* thresholds is *N*, we compute the following average area *S*.

$$S = \sum_{I=1}^{N} |R_I^L(u,v)| \quad (19)$$

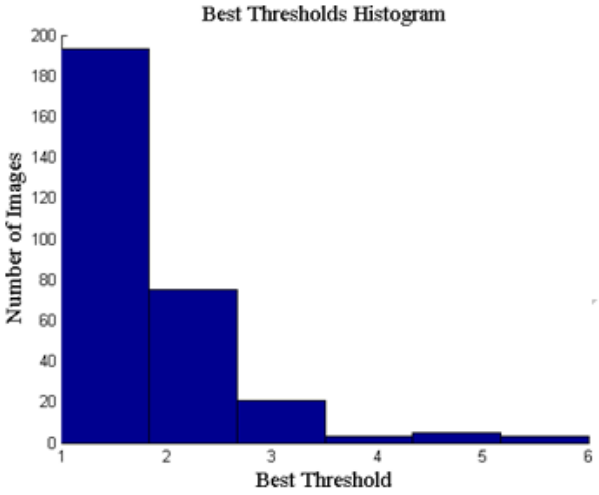

Fig. 4. Best threshold distribution for all 300 images from Berkeley database

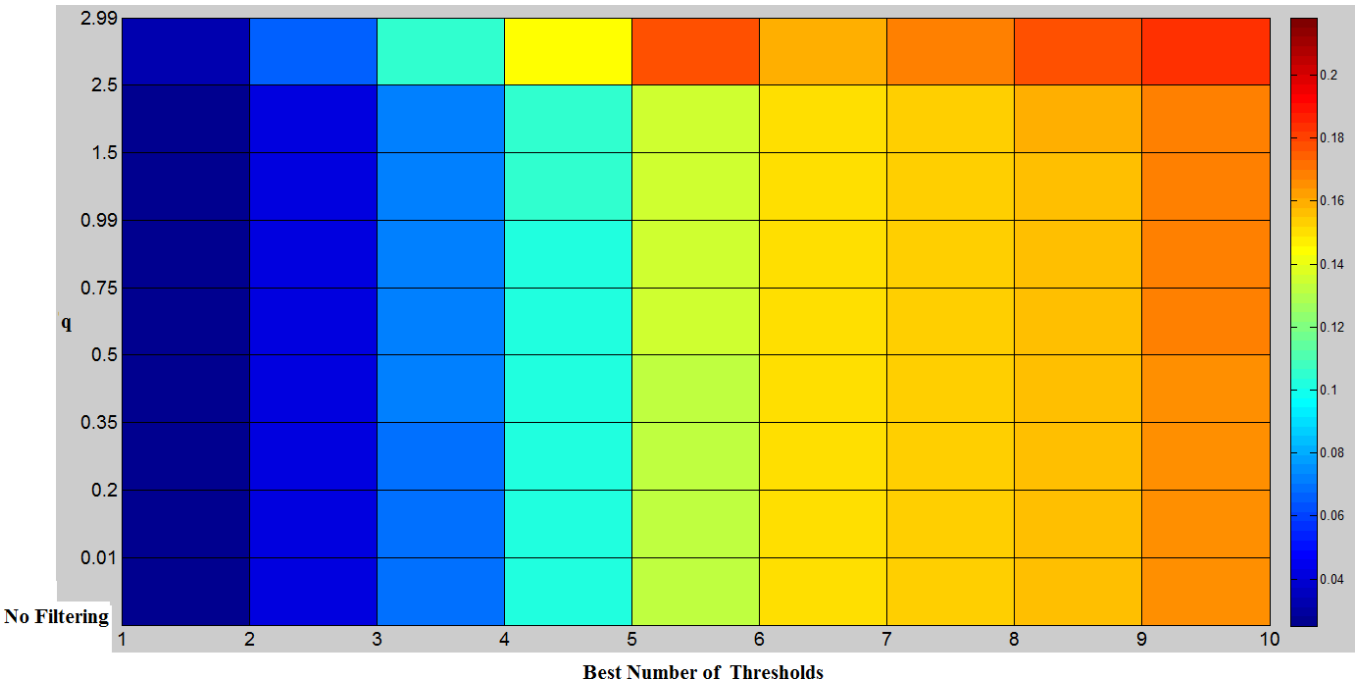

Fig. 5. Matrix of normalized distances for automatic and manual segmentation as a function of the number of thresholds and the *q* value of the pre-processing step with a *q*-gaussian filter.

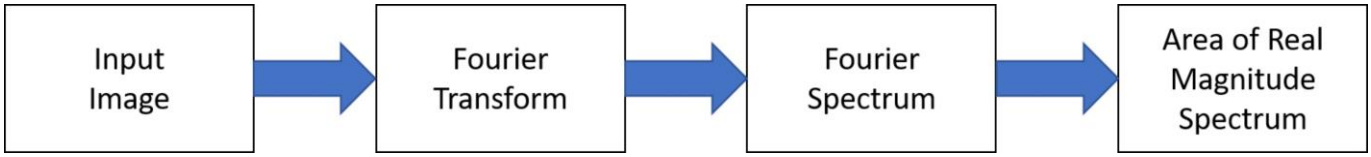

Fig. 6. Flowchart of experimental method to measure the correlation between an image's embedded components of frequency and the number of thresholds that best segment them.

Excluding the higher number of thresholds because they have been observed in a few images, one can observe that there is a strong correlation between the number of optimal thresholds for segmenting an image and the number of high frequencies embedded in an image. It suggests that the lower the number of high frequencies lower the number of thresholds to segment them; in other words: the higher the value of S smaller the presence of high frequencies in the set of images with this number of thresholds. Moreover, this behavior has an exponential decreasing as the number of thresholds to segment an image increase.

The result of Fig. 7 induces the observation of parameter correlation used in the experiments.

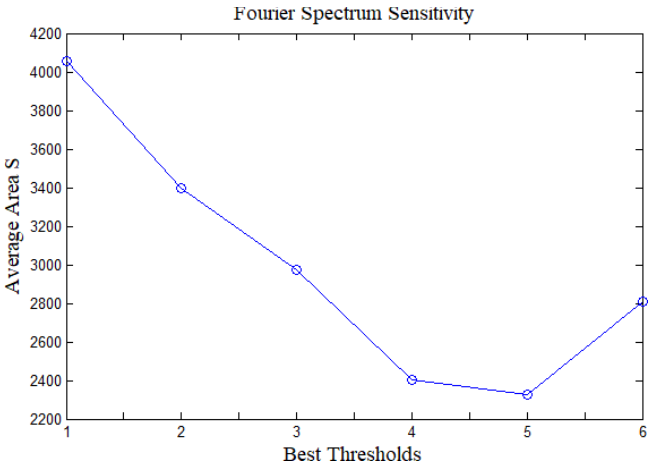

Fig. 7. Average variation for a set of images in the Berkeley database of the number of optimal thresholds with *S*.

Thus, the Table 1 shows the correlation between the three main parameters studied considering the following symbols adopted: *qtt* is value of the non-extensive parameter q used in the initial low-pass q-gaussian filtering; *#L* is the number of thresholds that minimizes the distance between the automatic image segmentation and its corresponding manual segmentation; and *#R* is the amount of high/low frequencies in a set of images.

VI. Conclusions

This paper presents a study of the number of thresholds for segmenting an image with a bio-inspired algorithm in a distributed process. The algorithm used was the Firefly meta-heuristic with a non-extensive entropic kernel. Each image was also pre-filtered with a spatial low-pass q-gaussian filter and the database for testing used 300 manually segmented images. The results showed that most of the images from the tested database needed fewer thresholds (up to 3) to get a multi-thresholding closer to the corresponding manually segmented images, and a much less amount required more than 3 up to 10 thresholds for the same purpose.

From this point, we hypothesize that the images with lower levels of embedded details are those that need fewer thresholds to meet the corresponding manual segmentation; and those with more embedded details need a much higher number of thresholds. To test this hypothesis, we compared the number of thresholds in the first part of the experiments with the spectrum of Fourier transformation of each image.

The results suggest that there is an inverse correlation between the value of Fourier spectrum and the number of thresholds need to approach an automatic segmentation to the corresponding ground truth; i.e., as greater the spectrum, smaller the number of required thresholds for segmenting an image, leaving the result closest to the ground truth. And when the spectrum has a low value, the number of thresholds is high.

TABLE I. CORRELATIONS BETWEEN THE PARAMETERS (*QTT* FOR THE GAUSSIAN SMOOTHING) *QTT*, NUMBER OF THRESHOLDS *#L* AND HIGH/LOW FREQUENCIES IN THE IMAGES *#R*.

	qtt	*#L*	*#R*
qtt	1.0	0.2289	-0.1951
#L	0.2289	1.0	-0.3181
#R	-0.1951	-0.3181	1.0

Since there is also an inverse positive correlation between the Fourier spectrum and the level of details in an image, the results indicate that there is also a correlation between a larger amount of details and the number of required thresholds. Thus, the spectrum of the Fourier transform may be a feature to be calculated in order to estimate the number of needed thresholds. However, the precise amount of this quantity, analytically computed between the spectrum value and the number of thresholds depends on more experiments and future studies.

References

[1] T. Pun, “Entropic thresholding: A new approach,” Comput. Graphics Image Process, vol. 16, pp. 210–239, 1981.

[2] J. N. Kapur, P. K. Sahoo, and A. K. C. Wong, “A new method for gray-level picture thresholding using the entropy of the histogram,” Comput. Graphics Image Process, vol. 29, pp. 273–285, 1985.

[3] A. S. Abutaleb, “A new method for gray-level picture thresholding using the entropy of the histogram,” Comput. Graphics Image Process, vol. 47, pp. 22–32, 1989.

[4] C. H. Li and C. K. Lee, “Minimum cross entropy thresholding,” Pattern Recognition, vol. 26, pp. 617–625, 1993.

[5] N. R. Pal, “On minimum cross entropy thresholding,” Pattern Recogni- tion, vol. 26, pp. 575–580, 1996.

[6] P. Sahoo, S. Soltani, A. Wong, and Y. Chen, “A survay of thresholding techniques,” Computer Vision Graphics Image Processing, vol. 41, no. 1, pp. 233–260, 1988.

[7] C.-I. Chang, Y. Du, J. Wang, S.-M. Guo, and P. Thouin, “Survey and comparative analysis of entropy and relative entropy thresholding techniques,” IEEE Proceedings, Vision, Image and Signal Processing, vol. 153, no. 6, pp. 837–850, Dec. 2006.

[8] M. P. Albuquerque, M. P. Albuquerque, I. Esquef, and A. Mello, “Image thresholding using tsallis entropy,” Pattern Recognition Letters, vol. 25, pp. 1059–1065, 2004.

[9] C. Tsallis, “Nonextensive statistics: Theoretical, experimental and computational evidences and connections,” Brazilian Journal of Physics, vol. 29, no. 1, March 1999.

[10] H. D. Cheng, J. Shan, W. Ju, Y. Guo, and L. Zhang, “Automated breast cancer detection and classification using ultrasound images: A survey,” Pattern Recognition, vol. 43, pp. 299–317, 2010.

[11] G. A. Giraldi, P. S. Rodrigues, C. E. Thomaz, and E. Kitani, “Statistical learning approaches for discriminate features selection,” Journal of the Brazilian Computer Society, vol. 20, pp. 1–16, 2008.

[12] P. S. Rodrigues, G. A. Giraldi, J. Suri, and R. F. Chang, “Non-extensive entropy for cad systems for breast cancer images,” in International Symposium on Computer Graphics and Image processing, SIBIGRAPI’06, I. C. Society, Ed., Manaus, 8-11 October 2006, pp. 121–128.

[13] J. S. Suri and R. M. Rangayyan, Recent Advances in Breast Imaging, Mammography and Computer Aided Diagnosis of Breast Cancer. SPIE Press, 2006.

[14] P. S. Rodrigues and G. A. Giraldi, “Improving Non-Extensive Medical Image Segmentation Based on Tsallis Entropy,” Pattern Analysis and Applications, vol. 14, no. 4, pp. 369–379, 2011.

[15] ——, “Computing the q-index for Tsallis Nonextensive Image Seg- mentation,” in Proceedings of the XXII International Simposium on Computer Graphics and Image Processing, PUC-RJ. Rio de Janeiro: IEEE Society, 2009, pp. 232–237.

[16] P. Rodrigues, G. Wachs-Lopes, H. Erdmann, M. Ribeiro, and G. Giraldi, “Improving a firefly meta-heuristic for multilevel image segmentation using tsallis entropy,” Pattern Analysis and Applications, pp. 1–20, 2015. [Online]. Available: http://dx.doi.org/10.1007/s10044-015-0450-x

[17] D. E. Goldberg, Genetic Algorithms in search, Optimization, and Ma- chine Learning. Reading, MA: Addison Wesley, 1997.

[18] S. Kirkpatrick, C. Gellat-Jr., and M. Vecchi, “Optimization by simulated annealing,” Science, no. 220, pp. 671–680, 1983.

[19] F. Glover, “Tabu search,” PART I, ORSA Journal of Computing 1, pp. 190–206, 1989.

[20] M. Dorigo, “Optimization, learning, and natural algorithms,” Ph.D. Thesis, Dipartimento di Elettronica e Informazione, Politecnico di Milano, Italy, 1992.

[21] J. Kennedy and R. C. Goldberg, “Particle swarm optimization,” in Proceedings of IEEE International Conference on Neural Networks, vol. IV, 1997, pp. 1942–1948.

[22] P. Y. Yin, “Multilevel minimum cross entropy threshold selection based on particle swarm optimization,” Applied Mathematics and Computation, vol. 184, pp. 503–513, 2007.

[23] S. Lukasik and Zak, “Firefly algorithm for continuous constrained optimization tasks,” in 1st international conference on computational collective intelligence, semantic web, 5-7 October 2009.

[24] X. S. Yang, “Firefly algorithms for multimodal optimization,” in Stochastic algorithms: Fundation and applications, SAGA 2009. Lecture notes in computer science, 2009, vol. 5792, pp. 169–178.

[25] M. H. Horng and R. J. Liou, “Multilevel minimum cross entropy threshold selection based on firefly algorithm,” Expert Systems with Applications, vol. 38, pp. 14 805–14 811, 2011.

[26] A. H. M. P. Tavares, “Aspectos matemáticos da entropia,” Master Thesis, Universidade de Aveiro, 2003.

[27] P. S. Rodrigues and G. Giraldi, “Improving the non-extensive medical image segmentation based on tsallis entropy,” Pattern Analysis and Applications (Print), vol. 14, pp. 1–18, 2011.

[28] H. Erdmann, G. A. Wachs-Lopes, M. P. Ribeiro, and P. S. Rodrigues, A study of a firefly meta-heuristics for multithreshold image segmentation. CRC Press, 2013, ch. 37, pp. 211–217.

[29] H. Erdmann, G. Wachs-Lopes, C. Galla˜o, M. P. Ribeiro, and P. S. Rodrigues, A Study of a Firefly Meta-Heuristics for Multithreshold Image Segmentation. Cham: Springer International Publishing, 2015, pp. 279–295. [Online]. Available: https://doi.org/10.1007/978-3-319- 13407-9 17

[30] P. S. Rodrigues, G. A. Wachs-Lopes, H. R. Erdmann, M. P. Ribeiro, and G. A. Giraldi, “Improving a firefly meta-heuristic for multilevel image segmentation using tsallis entropy,” Pattern Analysis and Applications, vol. 20, no. 1, pp. 1–20, Feb 2017. [Online]. Available: https://doi.org/10.1007/s10044-015-0450-x

[31] E. P. Borges, “Manifestações dinâmicas e termodinâmicas de sistemas não-extensivos,” PhD Thesis, Centro Brasileiro de Pesquisas Físicas, Rio de Janeiro, 2004.

[32] C.D.Gallao, “Aplicações de Funções q-Gaussianas no Processamento de Imagens Digitais,” Tese de Doutorado, Fundac¸a˜o Educacional Inaciana Pe. Sabo´ia de Medeiros, Sa˜o Paulo, A ser apresentada em Dezembro de 2015.

[33] D. Martin, C. Fowlkes, D. Tal, and J. Malik, “A database of human segmented natural images and its application to evaluating segmentation algorithms and measuring ecological statistics,” in Proc. 8th Int’l Conf. Computer Vision, vol. 2, July 2001, pp. 416–423.

[34] M. Sezgin and B. Sankur, “Survay ove image thresholding techniques and quantitative performance evaluation,” Journal of Eletronic Imaging, vol. 13, no. 1, pp. 146–165, 2004.